Effect of Humidity on the Interaction of CO_2 with Alkaline Anion Exchange Membranes Probed using the Quartz Crystal Microbalance

V.J. Bharath[1], J.R. Jervis[1], J. Bailey[1], E.C. Engebretsen[1], T. P. Neville[1, 2], J. Millichamp[1], T. Mason[1], P.R. Shearing[1], R. J. C Brown[3], G Manos[1], D. J. L. Brett[1]*

[1]Electrochemical Innovation Lab, Department of Chemical Engineering, University College London, Torrington Place, London, WC1E 7JE, UK

[2]Centre for Nature Inspired Engineering, University College London, Torrington Place, London, WC1E 7JE, UK

[3]National Physical Laboratory, Teddington, Middlesex, UK, TW11 0LW

Highlights

Membrane hydration shown to affect AAEM interaction with CO_2

Increasing hydration results in greater loss of membrane conductivity.

Pore opening and pore swelling have different regimes of CO_2 interaction.

Opening of membrane pore network leads to increasing CO_2 uptake.

Abstract

1. Introduction

Alkaline anion exchange membranes (AAEMs) are promising electrolyte materials for low temperature fuel cells [1, 2]. The AAEM has the benefit of facile oxygen reduction reaction (ORR) kinetics, and so does not require precious metal electrocatalysts [3-7]. The AAEM also has a solid polymer electrolyte (SPE) and so can be incorporated into compact designs, as seen with acid based proton exchange membrane (PEM) fuel cells [8, 9].

Compared to the aqueous alkaline fuel cell (A-FC), the AAEM-FC is much more portable and does not suffer from weeping of caustic electrolyte and leaking issues [8]; however, it is still susceptible to carbonate formation [10-13]. In A-FCs, metal carbonates form from the interaction of carbon dioxide in the air and metal cations within the aqueous electrolyte, such as K^+ and Na^+, as described in Equation 1 [8]. These metal carbonates precipitate and not only decrease the available OH^- ions but also form layers on the electrode surfaces, blocking active sites, gas diffusion layers (GDLs) and significantly reducing system performance.

$$CO_{2(g)} + 2OH^-{}_{(aq)} \rightarrow CO_3^-{}_{(aq)} + H_2O_{(l)} \tag{1}$$
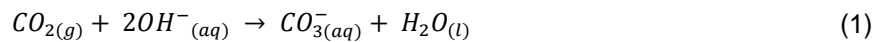
The AAEM has immobilised cationic functional groups tethered to its polymer backbone and thus the effect of carbonate formation on the system's ionic performance has been a topic of much debate. The membrane is still expected to form immobilised metal carbonates; however, these are thought to have minimal deleterious performance effects on fuel cell operation as they could not dissociate from the ionomer backbone and cause the aforementioned issues seen in the A-FC [14, 15]. Some studies have shown that the presence of carbonate ions can in fact improve fuel cell chemical stability and thus long-term operation [13, 14]; whilst others have presented opposing results, through a reduction in both ionic conductivity and its impact on the hydrogen oxidation reaction (HOR) [16-20].

Investigations have proven that the ionomer can operate in the carbonate (CO_3^{2-} / HCO_3^-) form [19]; however, the reported conductivities have been significantly lower when compared to operation in the OH^- form [21]. Varcoe *et al.* [13] has presented a potential solution, known as the self-purging mechanism, in which a humidified system can return to OH^- operation having been in the carbonate form. This mechanism requires the system to run at high current densities and in CO_2 free conditions; allowing the carbonate ions to be replaced by OH^- ions generated at the anode [16].

Even with promising commercialisation prospects, the effect of CO_2 interaction, membrane degradation and poor understanding of the system's hydration mechanisms, have resulted in very few commercially available AAEMs and thus no industry leading standard (such as Nafion in the case of acid based membranes). Many examples in the literature are conducted on in-house fabricated membranes; generally at the lab scale development stages and hence have huge discrepancies in findings, such as conductivity and thermal and chemical stability [8].
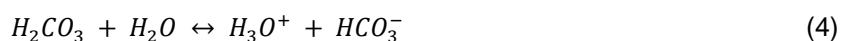
Tokuyama Co (Japan) has developed AAEMs that provides an ionic conductivity more comparable to that of Nafion, but little is known of the properties of the membranes or how they function in different operating conditions. Published work by Tokuyama and specifically Yanagi and Fukuta [19], has shown that the membrane is in fact hindered by operation in air, resulting in reduced conductivity in the A201 membrane from 42 mS cm^{-1} in the OH$^-$ form to 10 mS cm^{-1} in the carbonate form.

The investigation presented by Yanagi and Fakuta monitored the concentration of the anion species after exposure to ambient air from N_2 using Cl$^-$ ion exchange and titration based on the Warder method [19]. The results indicate that the absorption of CO_2 by the (wet) system was very fast and all OH$^-$ anions were converted to a combination of the carbonate (CO_3^{2-} / HCO_3^-) form within 30 mins [19].

The findings presented by Yanagi and Fakuta can be further explained as the introduction of CO_2 can dissolve into a humidified AAEM system and form a chemical equilibrium with carbonic acid, as shown in Equation 2; the CO_2 can also react directly with the inherent OH$^-$ ions in the system, as shown in Equation 3:

$$CO_{2(g)} + H_2O_{(l)} \leftrightarrow H_2CO_{3(aq)} \tag{2}$$

$$CO_{2(aq)} + OH^- \leftrightarrow HCO_3^- \tag{3}$$

Carbonic acid can be considered a diprotic acid and can therefore form hydrogen carbonates in the presence of H_2O (Equation 4) and carbonates containing CO_3^{2-} (Equations 5 and 6) [22].

$$H_2CO_3 + H_2O \leftrightarrow H_3O^+ + HCO_3^- \tag{4}$$

$$HCO_3^- + H_2O \leftrightarrow H_3O^+ + CO_3{}^{2-} \qquad (5)$$

$$HCO_3^- + OH^- \leftrightarrow H_2O + CO_3{}^{2-} \qquad (6)$$

Equations 2 – 6 show that the introduction of CO_2 into an AAEM system will not only form carbonate ions that may attach to the polymer's tethered cationic active sites, but also lowers the pH as the system becomes more acidic, as well as consuming OH^- ions reducing membrane conductivity and hence performance.

Water management and ionomer hydration plays a key role in effective fuel cell operation, including ionic conductivity [23] and ionomer degradation [Ref]. Equations 2 – 6 show that water may also play a key role in the mechanisms involved in reducing fuel cell performance through interaction with CO_2. It is therefore crucial that we understand how the system's humidity affects the degradation processes discussed above.

This work examines how reactant humidity (and hence membrane hydration) affects how CO_2 interacts with an AAEM. The change of membrane conductivity with exposure to air (as a source of CO_2) is compared with the change in viscoelastic properties of a thin-film ionomer, both as a function of humidity. The effect of CO_2 on the membrane material as a function of hydration is correlated with the solvation and swelling regimes and thus the access of CO_2 to the ionic channels within the membrane.

2. Experimental

2.1 Ex-situ resistance measurement

For this study, a commercially available alkaline anion exchange sheet membrane (A201, Tokuyama, Japan) was operated in an in-house fabricated closed-cathode fuel cell (5 cm^2 active area), with nitrogen running over both sides at a range of humidities. The A201 membrane was soaked in 1 M KOH for 5 hours to convert it from the Cl$^-$ form to the OH$^-$ form; it was then rinsed in deionised water, pat dried and inserted into the cell where it was held under stable conditions at 55 °C with 100 ml min^{-1} of N$_2$ (BOC) passing over each side. Using electrochemical impedance spectroscopy (EIS), the high-frequency intercept with the real axis of the Nyquist plot was used to determine the resistance of the system. Once the EIS high frequency intercept was constant, the supply of nitrogen was switched to air (at the same relative humidity), and the corresponding high frequency measurement recorded until stable. This process was repeated at a range of relative humidities (RHs) delivered using a calibrated dew point humidifier (Arbin, USA).

The membrane's transient high frequency intercept was measured using an IviumStat (Alkatek, UK). Impedance spectroscopy was measured potentiostatically at open circuit voltage, 0 V, with an AC amplitude of 10 mV; the amplitude was the smallest system perturbation which initiated a clear current response. The high frequency impedance was measured at 35 kHz every second; determined by performing impedance sweeps between 100 kHz and 100 Hz to find the high frequency intercept before the introduction of air to the system. The impedance sweep was also performed at the end of each experiment to verify a negligible shift in the high frequency intercept.

2.2 In-situ QCM interfacial measurements

2.2.1   The quartz crystal microbalance

The QCM is a bulk acoustic wave (BAW) resonator that has many applications, including implementation as an *in-situ* microbalance with nanogram resolution [24, 25]. The QCM is made up of a piezoelectric material (quartz) sandwiched between two electrically conductive gold electrodes. The quartz resonates at a specific resonant frequency (a function of its dimensions and mass deposition on its electrodes) when a voltage is applied.

The Sauerbrey equation (Equation 7) can be used to relate a shift in the system's frequency with either an increase or loss in the attached mass on the microbalance surface:

$$\Delta f = \frac{-2 f_o^2 \, \Delta m}{A \sqrt{\mu_q \, \rho_q}}$$

(7)

Where Δf is the measured change in frequency, f_0 is the fundamental frequency of the microbalance, A is the active piezoelectric area, μ_q is the shear modulus and ρ_q the density of quartz, and Δm is the systems mass change.

The Sauerbrey equation assumes that the deposited mass on the electrodes is evenly distributed; oscillates rigidly [25, 26] and has the same density and transverse velocity of quartz. The frequency shift from a deposited mass at any radial distance from the centre of the microbalance is assumed to be equal regardless of location [24]. Finally, the acoustic wave is assumed to travel through the microbalance and propagate through the additional film.

The QCM has proved to be a versatile *in-situ* mass monitoring technique for the study of polymer interactions at a solid interface, offering nanogram mass resolution [27-29]. For this study, the commercial AAEM ionomer (Tokuyama, Japan) is drop cast onto the QCM surface creating a composite resonator, thus allowing the QCM to be operated as a true in-situ sensor

2.2.2   Ionomer Casting

The Tokuyama AAEM which contains $[R_4N^+]$ cationic head groups is affected by the interaction with CO_2 even at low concentrations [8, 19, 30]. So to prevent any unwanted interaction with CO_2 in air, the ionomer casting process was carried out in-situ and the experimental set-up was developed to preclude any unwanted CO_2. The rig is shown in Figure 1(a) and further described in [31]. Mass spectrometry data has been used to confirm all seals are air-tight and to show no presence of any undesired air components.

The commercially available AS-4 ionomer dispersed in isopropanol alcohol (Tokuyama, Japan) was cast by micro-pipette *in-situ* under a 100 ml min^{-1} stream of desiccated N_2 (BOC, UK) directly onto a 6 MHz, 14 mm, gold coated double-anchor QCM electrode (Inficon) within the humidification chamber (Figure 1(b)). The casting process for each experimental run was conducted at 0% relative humidity (RH) to eliminate the water content contribution to

the ionomer thickness calculations. The composite resonator was then held at 55 °C and 0% RH for 1 hour to allow the ionomer to anneal.

The ionomer thickness t_i was subsequently determined using the Sauerbrey Equation (7) and Equation 8 below [31]:

$$t_i = \frac{m_i}{A \, \rho_i} \tag{8}$$

Where m_i is the measured ionomer mass (Sauerbrey equation), A, is the active cast area and ρ_i the recast ionomer density.
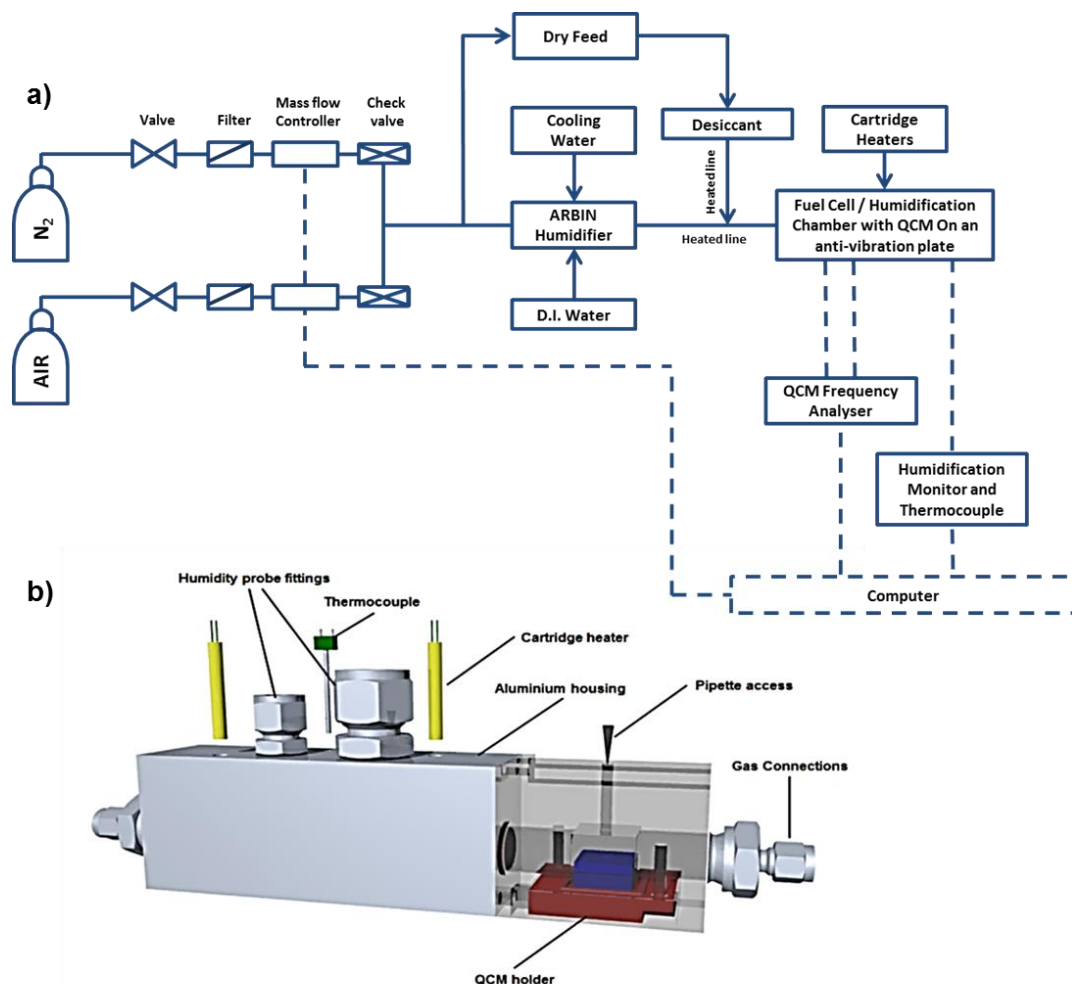

Figure 1: (a) Experimental rig setup allowing rapid switch over between nitrogen and air at the same dew point. (b) Shows the humidification chamber used throughout this investigation in which the composite resonator is both cast and operated.

This investigation uses thin film (65 ± 4 nm) drop cast ionomers for each study to ensure that the deposited mass is within the QCM's operable range [29], and to minimise contribution from internal water diffusion from the bulk when operating through the investigative range of relative humidities [28, 32, 33].

2.2.3 Composite resonator operation

After annealing, the composite resonator continues to operate under a nitrogen stream at 100 ml min^{-1} and 55°C; the same dew point humidifier was used to attain the system's relative humidity and is specific for each sub-investigation. The frequency was measured using a QCM200 controller (Stanford Research Systems, USA). Once the composite resonator achieved a stable frequency, the nitrogen was switched to a stream of air (BOC, UK) at the same flow rate and RH with ~ 400 ppm CO_2 concentration.

3. Results and Discussion

3.1 AAEM EIS resistance measurements

The first part of this investigation explores how humidity affects the high frequency ohmic resistance of a commercially available alkaline anion exchange sheet membrane (A201, Tokuyama) operating in atmospheric levels of CO_2 (air).

Figure 2 shows the % change in the measured high frequency resistance for A201 sheet AAEMs held at different RHs when operating in nitrogen (blue section) and subsequently in air of the same RH.
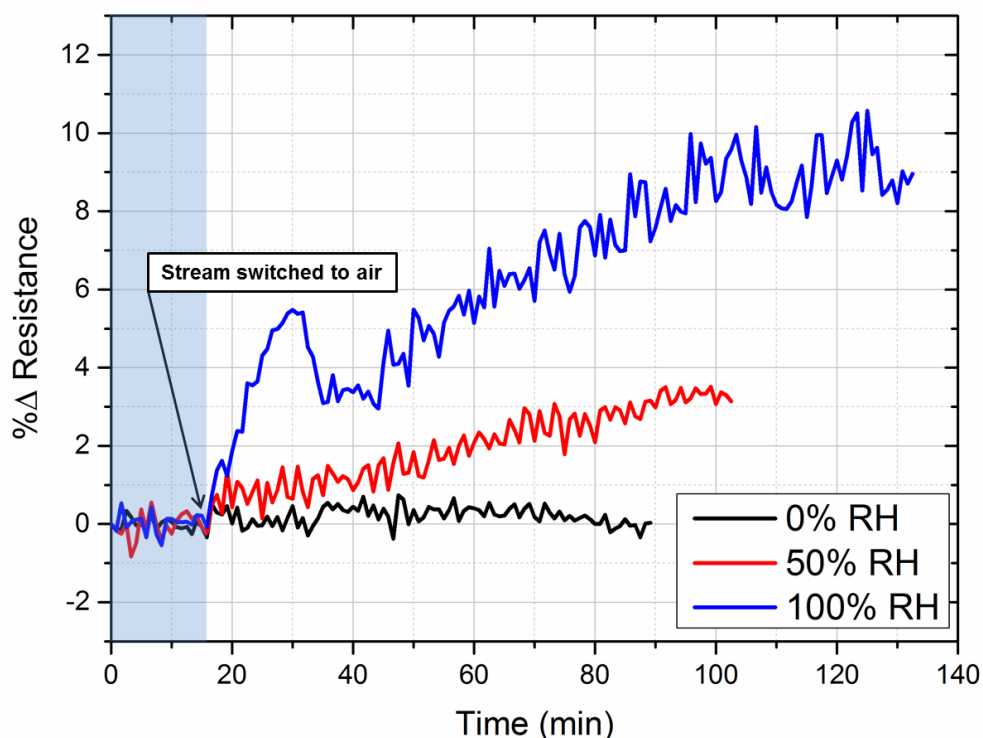

Figure 2: The % ohmic resistance change for the A201 membranes when operating in nitrogen (blue section) and subsequently in air containing atmospheric carbon dioxide at 0, 50 and 100% RH at 55 °C (represented as 50 second averaged intervals).

Figure 2 shows that when the AAEM is operated at 0% RH, there is no significant change in resistance when the operating conditions are changed from N_2 to air. However, at 50% and 100% RH, there is an increase in the membrane's resistance by 3.3% and 9%, respectively. It can also be seen that the transient response and associated stabilisation period of each

membrane increases with RH; this is expected as at higher RHs there is more activity in the membrane with increased water available and a potential equilibrium between liquid water formation and removal.

The effect of humidity on performance when operating in air has yet to be considered in the literature; however, decreases in performance when operating in air have been demonstrated elsewhere in functioning fuel cell systems [16, 34]. In functional fuel cell system studies however, the measured shifts in performance cannot solely be considered as an interaction with CO_2 because of other factors, including changing reactant partial pressures of the fuel stream ($O_2 \rightarrow$ air) during the switch over.

3.2 Quartz crystal microbalance response

The quartz crystal microbalance (QCM) has previously been used to examine the effect of water uptake and change in viscoelastic properties of thin-film AAEMs [31]. Here it is applied to examine the effect of AAEM interaction with CO_2 at different relative humidities.

Once cast and annealed at 0% RH, each drop-cast composite resonator was operated at a specific relative humidity, initially in nitrogen and subsequently in air (~400 ppm in CO_2); this was repeated for eight freshly cast QCM crystals operated through a relative humidity range of 0% - 88%. The processed frequency shift for each microbalance response is reported in f/f_0 (ppm) to normalise the specific resonant frequency and thus allow direct comparison between each investigation which has taken place on a different baseline due to each system being exposed to a different RH prior to introducing air (CO_2) [35].
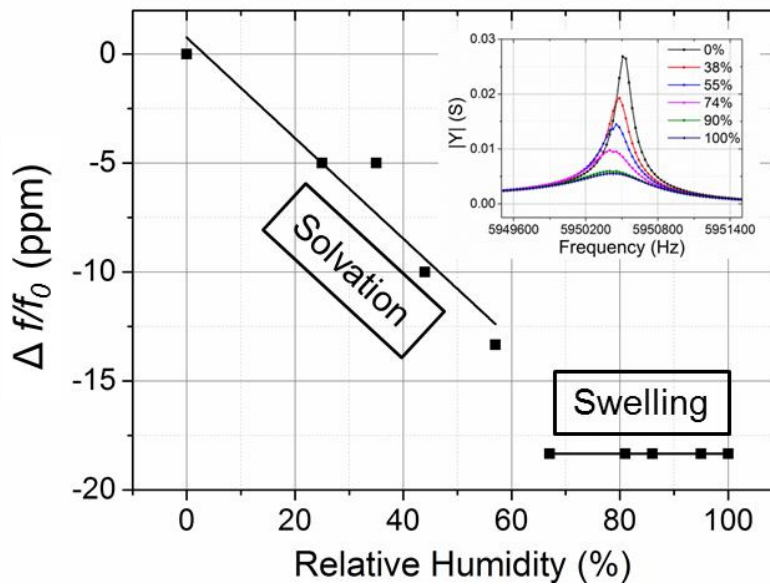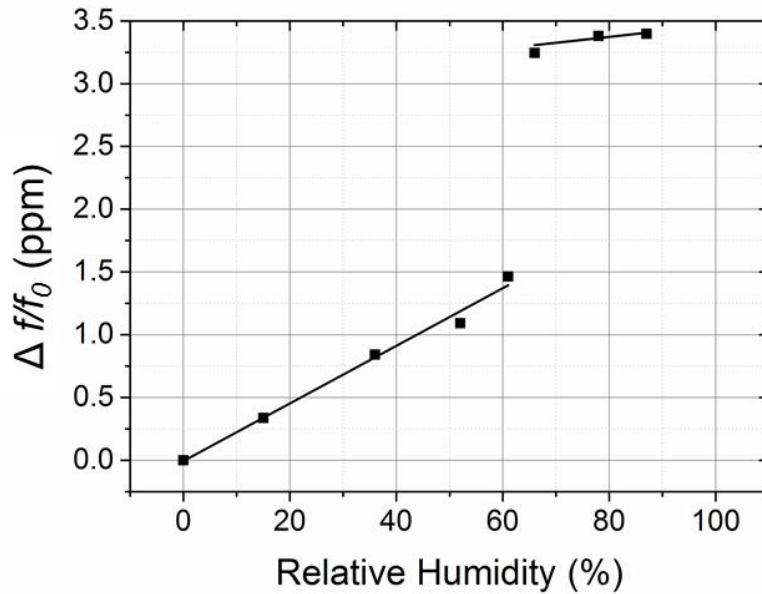
Figure 3: (a) Change in QCM frequency responses for composite resonators operating in nitrogen and subsequently in air at a range of RHs. (b) Shows the two AAEM hydration mechanisms determined through crystal admittance spectroscopy, discussed in [29]. The inset shows the measured Bode plot.

Figure 3(a) shows that at 0% RH, when there is no water in the system, there is no change in the composite resonator's resonant frequency. This agrees with the membrane resistance result in Figure 2 for 0% RH. In the range up to 62% RH, it can be seen that there is a linear increase with each resonator's absolute frequency shift with increasing RH. At 66% RH, the composite resonator shows a step change of 1.8 ppm from the investigation conducted at 62

% RH, and above 66% RH increasing RH has a significantly smaller effect on each of the composite resonator's frequency shifts.

Access of CO_2 to the pore network structure is expected to have an effect on the extent of interaction with the AAEM. As the RH is increased, it is possible that more CO_2 is able to permeate into the humidified membrane, allowing an increased production of carbonic acid within the system (Equation 2), which reacts with the hydroxyl anions (Equations 2 – 6) [19]. With increasing RH, the system becomes more acidic as the CO_2 uptake increases (and hence carbonate ion formation); the cationic head groups interact with the increased concentration of carbonate ions and results in an effective mass increase (frequency decrease). Figure 3(a) shows that the extent of CO_2 uptake increased linearly with humidity between 0 – 62% RH. At ~62% RH there is a significant step change which remains approximately constant between 66% and 88% RH.

The authors have previously described the hydration mechanisms in the AS-4 ionomer [31], the results of which are summarised by Figure 3(b). The findings suggest (through crystal admittance spectroscopy) that the ionomer initially undergoes a solvation period (< 66% RH) in which ion conducting channels begin to open, followed by swelling of these ionomer channels between 66% and 100% RH. There is a clear correlation between the degree of membrane hydration and the extent of CO_2 uptake. During the solvation regime (0 – 62% RH), the results suggest that the opening of membrane pores allows increasing access of CO_2 [29], and hence more interaction between cationic head group and carbonate ions. Once the channels are fully open (≥ 66% RH), all cationic sites become accessible as the ionomer is fully solvated and change in RH has little effect on CO_2 uptake.

4 Conclusion

Interaction of CO_2 with AAEMs is a potentially potent cause of performance degradation. Results here suggest that loss of membrane ion conductivity on exposure to CO_2 is a function of membrane hydration; increasing membrane hydration leads to more substantial resistance increases. Thin-film ionomer studies using the QCM has allowed for very accurate measurement of CO_2 uptake (carbonate formation) into the membrane. Exposing the cast membrane to atmospheric levels of CO_2 in air and operating at the typical operating temperature of the membrane in a device (55 °C), suggests that there is a correlation between CO_2 uptake and the level of hydration of the membrane; the pore opening regime resulting in a linear increase in CO_2 uptake as water permeates the pore system and cation headgroups become increasingly accessible to CO_2. The transition to the pore swelling phase sees a step increase in CO_2 uptake as the network is fully open and continues to swell with water but does not lead to an increase in CO_2 uptake with increasing RH.

5 References

[1] J.R. Varcoe, R.C.T. Slade, Prospects for alkaline anion-exchange membranes in low temperature fuel cells, Fuel Cells, 5 (2005) 187-200.

[2] M.A. Hickner, A.M. Herring, E.B. Coughlin, Anion Exchange Membranes: Current Status and Moving Forward (vol 51, pg 1727, 2013), J Polym Sci Pol Phys, 52 (2014) 347-347.

[3] R. Jervis, N. Mansor, C. Gibbs, C.A. Murray, C.C. Tang, D.J.L. Brett, Novel PdIr/C Catalysts for the Hydrogen Oxidation Reaction in Alkaline Media, Polymer Electrolyte Fuel Cells 13 (Pefc 13), 58 (2013) 637-650.

[4] R. Jervis, N. Mansor, C. Gibbs, C.A. Murray, C.C. Tang, P.R. Shearing, D.J.L. Brett, Hydrogen Oxidation on PdIr/C Catalysts in Alkaline Media, J Electrochem Soc, 161 (2014) F458-F463.

[5] S. Gu, R. Cai, T. Luo, Z.W. Chen, M.W. Sun, Y. Liu, G.H. He, Y.S. Yan, A Soluble and Highly Conductive Ionomer for High-Performance Hydroxide Exchange Membrane Fuel Cells, Angew Chem Int Edit, 48 (2009) 6499-6502.

[6] S.F. Lu, J. Pan, A.B. Huang, L. Zhuang, J.T. Lu, Alkaline polymer electrolyte fuel cells completely free from noble metal catalysts, P Natl Acad Sci USA, 105 (2008) 20611-20614.

[7] N.J. Robertson, H.A. Kostalik, T.J. Clark, P.F. Mutolo, H.D. Abruna, G.W. Coates, Tunable High Performance Cross-Linked Alkaline Anion Exchange Membranes for Fuel Cell Applications, J Am Chem Soc, 132 (2010) 3400-3404.

[8] G. Merle, M. Wessling, K. Nijmeijer, Anion exchange membranes for alkaline fuel cells: A review, J Membrane Sci, 377 (2011) 1-35.

[9] V. Mehta, J.S. Cooper, Review and analysis of PEM fuel cell design and manufacturing, J Power Sources, 114 (2003) 32-53.

[10] G.F. McLean, T. Niet, S. Prince-Richard, N. Djilali, An assessment of alkaline fuel cell technology, Int J Hydrogen Energ, 27 (2002) 507-526.

[11] M. Cifrain, K.V. Kordesch, Advances, aging mechanism and lifetime in AFCs with circulating electrolytes, J Power Sources, 127 (2004) 234-242.

[12] E. Gulzow, M. Schulze, Long-term operation of AFC electrodes with CO2 containing gases, J Power Sources, 127 (2004) 243-251.

[13] L.A. Adams, S.D. Poynton, C. Tamain, R.C.T. Slade, J.R. Varcoe, A carbon dioxide tolerant aqueous-electrolyte-free anion-exchange membrane alkaline fuel cell, Chemsuschem, 1 (2008) 79-81.

[14] J.A. Vega, C. Chartier, S. Smith, W.E. Mustain, Effect of Carbonate on Oxygen Reduction, Hydrogen Oxidation and Anion Exchange Membrane Chemical Stability, Polymer Electrolyte Fuel Cells 10, Pts 1 and 2, 33 (2010) 1735-1749.

[15] J.F. Zhou, M. Unlu, J.A. Vega, P.A. Kohl, Anionic polysulfone ionomers and membranes containing fluorenyl groups for anionic fuel cells, J Power Sources, 190 (2009) 285-292.

[16] F.K.I.H.W.S.Y. H, In-Situ Observation of CO2 through the Self-purging in Alkaline Membrane Fuel Cell (AMFC) Ecs Transactions, 23-27 (2009).

[17] Y. Matsui, M. Saito, A. Tasaka, M. Inaba, Influence of Carbon Dioxide on the Performance of Anion-Exchange Membrane Fuel Cells, Ecs Transactions, 25 (2010) 105-110.

[18] J.L. Yan, M.A. Hickner, Anion Exchange Membranes by Bromination of Benzylmethyl-Containing Poly(sulfone)s, Macromolecules, 43 (2010) 2349-2356.

[19] H. Yanagi, K. Fukuta, Anion Exchange Membrane and Ionomer for Alkaline Membrane Fuel Cells (AMFCs), Proton Exchange Membrane Fuel Cells 8, Pts 1 and 2, 16 (2008) 257-262.

[20] A. Tewari, V. Sambhy, M.U. Macdonald, A. Sen, Quantification of carbon dioxide poisoning in air breathing alkaline fuel cells, J Power Sources, 153 (2006) 1-10.

[21] T.P. Pandey, A.M. Maes, H.N. Sarode, B.D. Peters, S. Lavina, K. Vezzu, Y. Yang, S.D. Poynton, J.R. Varcoe, S. Seifert, M.W. Liberatore, V. Di Notob, A.M. Herring, Interplay between water uptake, ion

interactions, and conductivity in an e-beam grafted poly(ethylene-co-tetrafluoroethylene) anion exchange membrane, Phys Chem Chem Phys, 17 (2015) 4367-4378.

[22] A.H. England, A.M. Duffin, C.P. Schwartz, J.S. Uejio, D. Prendergast, R.J. Saykally, On the hydration and hydrolysis of carbon dioxide, Chem Phys Lett, 514 (2011) 187-195.

[23] Q.J. Duan, S.H. Ge, C.Y. Wang, Water uptake, ionic conductivity and swelling properties of anion-exchange membrane, J Power Sources, 243 (2013) 773-778.

[24] D.A. Buttry, M.D. Ward, Measurement of Interfacial Processes at Electrode Surfaces with the Electrochemical Quartz Crystal Microbalance, Chem Rev, 92 (1992) 1355-1379.

[25] G. Sauerbrey, Verwendung Von Schwingquarzen Zur Wagung Dunner Schichten Und Zur Mikrowagung, Z Phys, 155 (1959) 206-222.

[26] M. Rodahl, F. Hook, A. Krozer, P. Brzezinski, B. Kasemo, Quartz-Crystal Microbalance Setup for Frequency and Q-Factor Measurements in Gaseous and Liquid Environments, Rev Sci Instrum, 66 (1995) 3924-3930.

[27] G. Liu, G. Zhang, QCM-D studies on polymer behavior at interfaces, Springer, New York, 2013.

[28] A. Kongkanand, Interfacial Water Transport Measurements in Nafion Thin Films Using a Quartz-Crystal Microbalance, J Phys Chem C, 115 (2011) 11318-11325.

[29] J. John, K.M. Hugar, J. Rivera-Melendez, H.A. Kostalik, E.D. Rus, H.S. Wang, G.W. Coates, H.D. Abruna, An Electrochemical Quartz Crystal Microbalance Study of a Prospective Alkaline Anion Exchange Membrane Material for Fuel Cells: Anion Exchange Dynamics and Membrane Swelling, J Am Chem Soc, 136 (2014) 5309-5322.

[30] J.A. Vega, W.E. Mustain, Effect of CO_2, HCO_3^- and CO_3^{2-} on oxygen reduction in anion exchange membrane fuel cells, Electrochim Acta, 55 (2010) 1638-1644.

[31] V.J. Bharath, J. Millichamp, T.P. Neville, T.J. Mason, P.R. Shearing, R.J.C. Brown, G. Manos, D.J.L. Brett, Measurement of water uptake in thin-film Nafion and anion alkaline exchange membranes using the quartz crystal microbalance, J Membrane Sci, 497 (2016) 229-238.

[32] G.C. Abuin, M.C. Fuertes, H.R. Corti, Substrate effect on the swelling and water sorption of Nafion nanomembranes, J Membrane Sci, 428 (2013) 507-515.

[33] G.C. Abuin, P. Nonjola, E.A. Franceschini, F.H. Izraelevitch, M.K. Mathe, H.R. Corti, Characterization of an anionic-exchange membranes for direct methanol alkaline fuel cells, Int J Hydrogen Energ, 35 (2010) 5849-5854.

[34] G.W. Li, Y. Wang, J. Pan, J.J. Han, Q. Liu, X.Q. Li, P.C. Li, C. Chen, L. Xiao, J.T. Lu, L. Zhuang, Carbonation effects on the performance of alkaline polymer electrolyte fuel cells, Int J Hydrogen Energ, 40 (2015) 6655-6660.

[35] J. Millichamp, E. Ali, N.P. Brandon, R.J.C. Brown, D. Hodgson, C. Kalyvas, G. Manos, D.J.L. Brett, Application of a GaPO4 Crystal Microbalance for the Detection of Coke Formation in High-Temperature Reactors and Solid Oxide Fuel Cells, Ind Eng Chem Res, 50 (2011) 8371-8375.